Macromolecular Research, Vol. 21, No. 2, pp 228-233 (2013)
DOI 10.1007/s13233-013-1072-z

www.springer.com/13233
pISSN 1598-5032 eISSN 2092-7673

Colorless and Transparent Polyimide Nanocomposites: Thermo-Optical Properties, Morphology, and Gas Permeation

Youngmin Kim and Jin-Hae Chang*

School of Energy and Integrated Materials Engineering, Kumoh National Institute of Technology, Gyeongbuk 730-701, Korea

Received August 12, 2012; Revised October 26, 2012; Accepted November 2, 2012

Abstract: A series of colorless and transparent polyimide (PI) hybrid films was synthesized from bicyclo[2.2.2]oct-7-ene-2,3,5,6-tetracarboxylic dianhydride (BTDA) and bis[4-(3-aminophenoxy)phenyl] sulfone (m-BAPS) with various clay contents, by solution intercalation polymerization to poly(amic acid)s, followed by thermal imidization. The thermal properties, morphologies, optical transparencies, and gas permeations of the PI hybrid films were examined for organoclay loadings ranging from 0 to 40 wt%. Up to a clay loading of 20 wt%, the clay particles were found to be highly dispersed in the PI matrix without any agglomeration of particles. However, for a clay content above 20 wt% some agglomerated structures form in the polymer matrix. The thermal and oxygen barrier properties of the PI hybrid films were gradually improved by increasing the organoclay content from 0 to 40 wt%. However, the optical transparency of the PI hybrid films deteriorated with increasing organoclay content.

Keywords: colorless and transparent polyimide, film, nanocomposite, organoclay.

Introduction

Recently, much research effort has been devoted to developing high performance polyimide (PI) materials with excellent thermomechanical properties, good solubility, and high optical transparency.[1-4] In particular, colorless PIs have been prepared using dianhydride and diamine monomers substituted with fluorine moieties in their side groups.[5-8] Moreover, these colorless and transparent PIs were shown to have solubility, thermal stability, and optical transparency characteristics superior to those of other commercialized PIs. Optically colorless and transparent PI films have many potential uses in electro-optical devices, flexible display substrates, and semiconductor applications.[9-13]

Previous studies have demonstrated that a high-performance nanocomposite PI material with organoclay can be synthesized by thermal imidization of an aromatic precursor polymer.[14-16] Nanostructured materials often possess a combination of physical and mechanical properties not present in conventional composites. Even at low clay contents (<10 wt%), the thermomechanical properties of nanostructured materials can be substantially increased while decreasing their gas permeability rate.[17-19]

We also previously reported the preparation of colorless and transparent PI hybrid films containing low clay content highly dispersed in *N*,*N*-dimethylacetamide (DMAc) by using 4,4'-(hexafluoroisopropylidene) diphthalic anhydride (6FDA) and diamines designed to introduce ether or sulfone linkages into the polymer main chain, thereby considerably increasing the transparency of PIs without decreasing their thermal stability.[17,20,21]

We prepared a series of colorless and transparent PI hybrid films composed of a PI and an excess of organoclay, Cloisite 30B (≤40 wt%), by thermal imidization of an aromatic precursor polymer synthesized based on the reaction of bicyclo[2.2.2]oct-7-ene-2,3,5,6-tetracarboxylic dianhydride (BTDA) and bis[4-(3-aminophenoxy)phenyl] sulfone (m-BAPS). The introduction of BTDA and m-BAPS into PI containing bent structures modifies their thermo-optical properties and gas permeation because of the effects on charge transfer complex (CT-complex) formation.

The objective of this study was to evaluate the effect of the organoclay in PI nanocomposites, as a hybrid system, as a function of the amount of organoclay. In this paper, we describe a method for producing the colorless and transparent PI hybrids by using solution intercalation. The thermal properties, morphologies, and optical transparencies of the PI hybrid films are reported for various organoclay contents. The oxygen barrier properties of the hybrid films were also studied, and the film form was evaluated as a function of the organoclay content in the PI matrix polymer.

Experimental

Materials. Cloisite 30B (organically modified montmorillonite (MMT)) was obtained from Southern Clay Products, Inc.

*Corresponding Author. E-mail: changjinhae@hanmail.net

The reagents were purchased from TCI (Tokyo, Japan) and Aldrich Chemical Co. (Yongin, Korea). BTDA and m-BAPS were obtained from TCI and used as received. DMAc was purified and dried over molecular sieves before use. All other reagents were used without further purification.

Preparation of Colorless PI Hybrid Films. Poly(amic acid) (PAA) was synthesized from BTDA and m-BAPS in DMAc at a low temperature. BTDA (5.72 g; 1.32×10^{-2} mol) and DMAc (30 mL) were placed in a 100-mL three-necked flask, and the mixture was stirred at 0 °C for 30 min under a nitrogen atmosphere. m-BAPS (3.28 g; 1.32×10^{-2} mol) in DMAc (24 mL) was then added. The resulting solution was stirred vigorously at 0 °C for 1 h and then at room temperature for 14 h, yielding a 14 wt% DMAc solution of PAA.

The procedures used to prepare the polymer/organoclay hybrids were the same for all organoclay contents, so here we only describe the preparation of PI hybrid containing 10 wt% Cloisite 30B as a representative example. A dispersion of 1 g Cloisite 30B, 63 g PAA solution, and excess DMAc (10 mL) was stirred vigorously at room temperature for 2 h to achieve better dispersion. Cloisite 30B was used for producing our hybrid films because it has outstanding dispersibility in DMAc. The solution was cast onto glass plates, and then, the solvent was evaporated at 50 °C for 1 h. The films were then dried in a vacuum oven at 80 °C for 1 h. The PAA films were further imidized on the glass plates through sequential heating at 100, 130, 160, 190, and 220 °C for 30 min at each temperature and under various pressure conditions, followed by heating at 250 °C for 30 min. Fixed tools were not used to orient the films on the glass plates during heat treatment because orientation can affect some characteristics, such as optical properties and morphology, of film specimens.

Table I lists the thermal imidization conditions used in the preparation of the PI hybrid films. The chemical structures relevant to the synthetic route are shown in Scheme I. We attempted to synthesize a PI hybrid film containing more than 40 wt% organoclay. However, repeated attempts to polymerize the 50 wt% Cloisite 30B/PI hybrid failed because of bubbles produced in the polymerization reactor. Excess organoclay in the PI hybrid containing 50 wt% Cloisite 30B appeared to prohibit the production of the PI hybrid film.

Characterizations. Wide-angle X-ray diffraction (XRD) measurements were performed at room temperature on a Rigaku (D/Max-IIIB) X-ray diffractometer by using Ni-filtered CuK_α radiation. The scanning rate was 2°/min over the range 2θ= 2°-12°. A differential scanning calorimeter (DSC 200F3) was used on a NETZSCH instrument, and a thermogravimetric analyzer (Auto TGA 1000) was used on a TA instrument with a heating rate of 20 °C/min under N_2 flow. The coefficients of thermal expansion (CTEs) of the samples were measured with a macro-expansion probe (TMA-2940), which was used to apply a 0.1 N expansion force to the films at a heating rate of 5 °C/min in the 40-190 °C range.

Table I. Synthetic Conditions of PI Hybrid Films

Conditions	Temperature (°C)/Time (h)/Pressure (Torr)
PAA	0/1/760 → 25/14/760
PAA Hybrid	25/2/760 → 50/1/760 → 80/1/1
Thermal Imidization	100/0.5/1 → 130/0.5/760 → 160/0.5/760→ 190/0.5/760 → 220/0.5/760 → 250/0.5/760

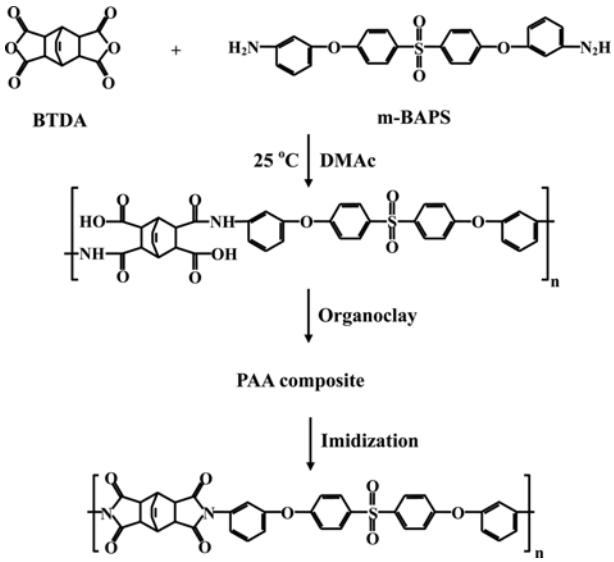

Scheme I. Synthetic route of PI nanocomposite.

Transmission electron microscopy (TEM) photographs of ultrathin sections of the PI hybrid films were obtained with a LEO 912 OMEGA transmission electron microscope by using an acceleration voltage of 120 kV. The color intensities of the polymer films were evaluated with a Minolta spectrophotometer (Model CM-3500d). The ultraviolet-visible (UV-vis) spectra of the polymer films were recorded on a Shimadzu UV-3600 instrument. The O_2 permeabilities of the films were measured based on ASTM E96 by using a Mocon DL 100. The O_2 transmission rates were obtained at 23 °C under 1 atm pressure.

Results and Discussion

XRD. Figure 1 shows the XRD curves for the organoclay, Cloisite 30B, in the region with 2θ of 2° to 12°. The reflection of Cloisite 30B was found at 2θ=4.78° (d=18.50 Å). Figure 1 also shows the XRD curves for the pure PI and the PI hybrid films with various clay contents in the range of 0 to 40 wt%.

Very weak peaks at 2θ=2.97° (d=29.72 Å) and 5.96° (d= 14.83 Å) were found in the XRD results for the 10 wt% PI hybrid. A second XRD peak observed at 2θ=5.96° corresponds to the (002) plane of the organoclay layers. Similar XRD peaks are shown for the PI hybrid with 20 wt% organoclay content. The intensity of the XRD peaks at 2θ=2.97° and 5.96°, however, increased suddenly as the clay loading was

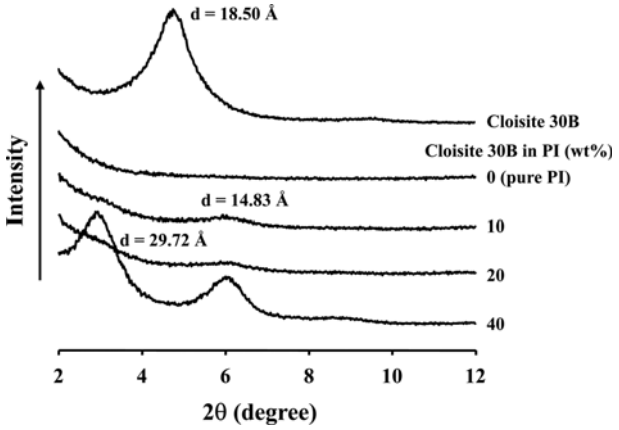

Figure 1. XRD patterns of Cloisite 30B and PI hybrids with various Cloisite 30B contents.

increased from 20 to 40 wt%, suggesting that dispersion is more effective for lower clay loadings than for higher ones. Higher clay loadings are expected to increase the agglomeration of some portion of the clay within the PI matrix; however, the presence of the organoclay was found to have no effect on the location of the peak, which indicates that perfect exfoliation of the clay layer structure of the organoclay does not occur in the PI matrix.

XRD offers a convenient way to determine the interlayer spacing due to the periodic arrangement of silicate layers in the virgin clay and in intercalated layered hybrids. Although XRD enables precise routine measurements of clay layer spacings, it does not enable the spatial distributions of clay layers to be determined, nor does it enable any structural inhomogeneities in the hybrids to be detected. In addition, some layered clays do not initially exhibit well-defined basal reflections, so peak broadening and intensity decreases are difficult to follow systematically. Thus, conclusions concerning the mechanisms of hybrid formation and microstructure, based solely on XRD results, are only tentative.[22,23] Further evidence of the clay dispersion in the PI films on a nanometer scale was obtained with TEM.

Morphology. To more precisely examine the dispersion of the clay layers in the PI hybrids, we carried out TEM studies. TEM affords a qualitative understanding of the internal structure through direct observation. Typical TEM photographs of the hybrids with organoclays are displayed in Figure 2. Figure 2(a) shows the TEM photographs of the PI hybrids containing 20 wt% Cloisite 30B. The dark lines in these images are the 1-nm-thick clay layers, the spaces between the dark lines are interlayer spaces, and the gray bases are the PI matrix. For the Cloisite 30B hybrids shown in Figure 2(a), some of the clay is dispersed well throughout the PI matrix, and some of it is agglomerated to approximately 10-20 nm. As in the case of the 40 wt% Cloisite 30B (Figure 2(b)), these clays are for the most part agglomerated in the polymer matrix. The presence of peaks in the XRD patterns of

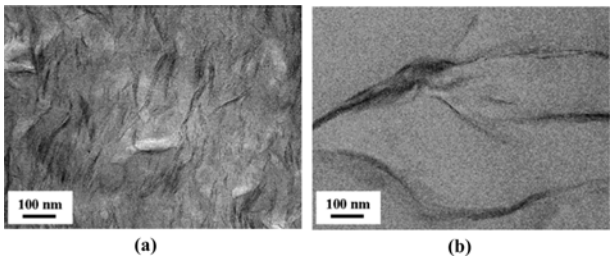

Figure 2. TEM micrographs of PI hybrid films containing (a) 20 and (b) 40 wt% Cloisite 30B.

Table II. Thermal Properties of PI Hybrid Films

Organoclay (wt%)	T_g (°C)	$T_D^{i\,a}$ (°C)	$wt_R^{600\,b}$ (%)	CTE^c (ppm/°C)
0 (pure PI)	228	385	34	66
10	235	397	42	54
20	242	405	45	47
40	238	481	85	35

[a]At a 2% initial weight-loss temperature. [b]Weight percent of residue at 600 °C. [c]Coefficient of thermal expansion for 2nd heating is 50-150 °C.

these samples can be attributed to the agglomerated layers (Figure 1). Unlike the clay layers of the 20 wt% Cloisite 30B hybrids, those of the 40 wt% hybrid are not intercalated into the matrix polymer, consistent with the XRD data in Figure 1. It is clear from the figure that the agglomeration of the dispersed clay phase increases with the clay content. It is conceivable that the agglomerated clay domain may deteriorate the thermal properties and decrease the optical transparencies of the hybrids, probably because of poor interfacial adhesion between the organoclay and the PI hybrid matrix.

Thermal Behavior. Table II presents the thermal properties of the pure PI and the PI hybrid films with various organoclay contents. The glass transition temperatures (T_g) of the PI hybrids increase from 228 to 242 °C with increasing clay loading from 0 to 20 wt%. This increase in T_g is ascribed to the confinement of the intercalated polymer chains within the clay galleries, which prevents segmental motions of the polymer chains.[24-26] However, the glass transition temperatures of the PI hybrids increase with the addition of clay only up to a critical loading and then decrease above that. For example, when the organoclay content reaches 40 wt%, T_g is 238 °C. This decrease in T_g seems to be the result of clay agglomeration, which occurs upon the addition of clay into the polymer matrix above the critical loading. The DSC thermograms of the pure PI and the hybrids are shown in Figure 3.

The initial thermal degradation temperature (T_D^i) values of the PI hybrid films increase significantly from 385 to 481 °C as the organoclay loading is increased from 0 to 40 wt% (Table II). For example, the T_D^i value of the PI hybrid film with a 40 wt% clay loading (481 °C) is higher than that

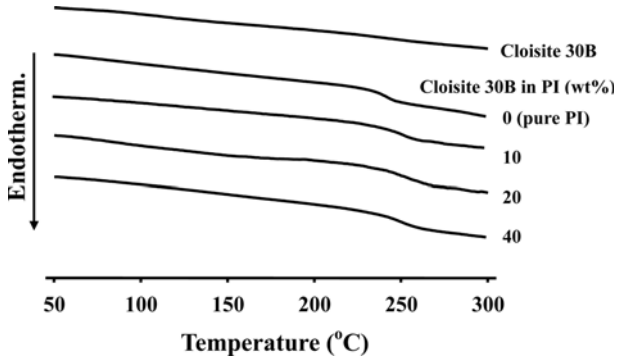

Figure 3. DSC thermograms of PI hybrids with various Cloisite 30B contents.

of the pure PI (385 °C) by 96 °C. The presence of the clay increases the T_D^i value by acting as an insulator and as a mass-transport barrier to the volatile products generated during decomposition.[27,28] This increase in the thermal stability is also due to the high thermal stability of the clay and the interactions between the clay particles and the polymer matrix. The weight of the residue at 600 °C was also found to increase gradually for clay loadings between 0 and 40 wt%, from 34% to 85%, as shown in Table II. This enhancement in char formation is ascribed to the high heat resistance of the clay itself. The thermal stabilities of the PI hybrids with various clay loadings are plotted in Figure 4.

The CTEs of the PI hybrids in the temperature range 50-150 °C decrease with the addition of clay up to 40 wt%, as listed in Table II. For example, the CTEs of the PI hybrids decrease from 66 to 35 ppm/°C with increasing clay loading from 0 to 40 wt%. This observation suggests that the amount by which thermal expansion of the clay layers is reduced depends on the orientation of the PI molecules and the rigid nature of the clay layers. Upon heating, the in-plane-oriented PI molecules tend to relax in a direction normal to their

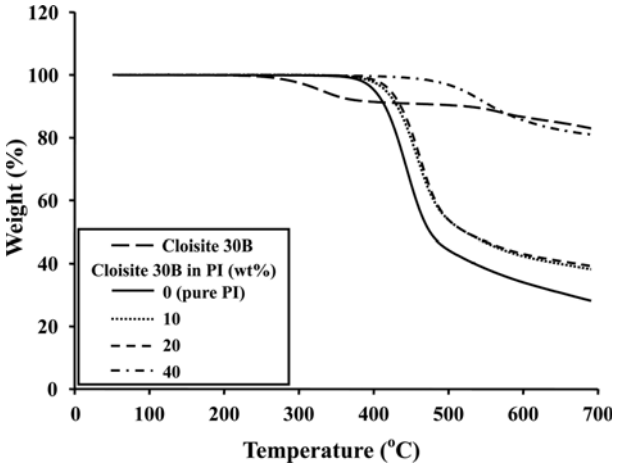

Figure 4. TGA thermograms of PI hybrids with various Cloisite 30B contents.

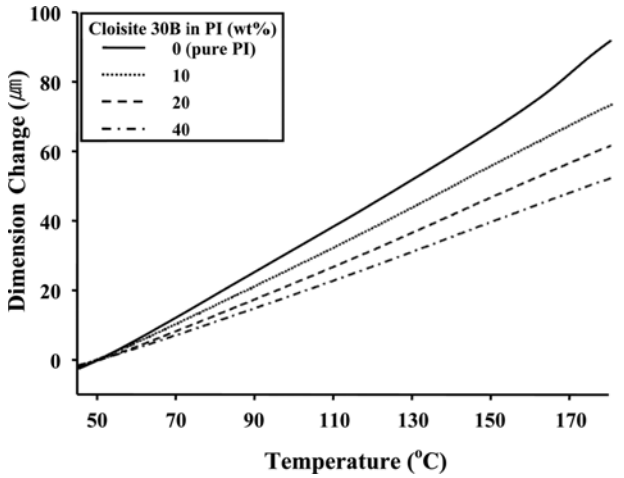

Figure 5. TMA thermograms of PI hybrids with various Cloiste 30B contents.

Table III. Optical Properties of PI Hybrid Films

Organoclay (wt%)	Thickness (μm)	λ_0[a] (nm)	$550_{nm}^{trans.}$ (%)	Y.I.[b]
0 (pure PI)	80	298	87	2.35
10	68	307	80	5.63
20	67	311	80	6.23
40	70	316	75	13.15

[a]Cutoff wavelength. [b]Yellow index.

original orientation, and thus, expand mainly in the out-of-plane direction.[29,30] The clay layers are much more rigid than the PI molecules, so they do not deform or relax as easily. As a result, the clay layers retard the thermal expansion of the PI molecules very effectively in the out-of-plane direction. The CTE results on second heating for the PI hybrid films with various Cloisite 30B contents are shown in Figure 5.

Optical Transparency. The optical properties of the PI hybrid films with various Cloisite 30B contents are listed in Table III. The color intensities of the hybrid films were also determined from the cutoff wavelength (λ_0) in the UV-vis absorption spectra, as shown in Figure 6. λ_0 values of the PI hybrids increase linearly with increasing organoclay loading, from 298 to 316 nm when the Cloisite 30B content is increased from 0 to 40 wt%, because of agglomeration of the clay particles. The hybrid films with 0-40 wt% organoclay content exhibit a UV transmittance in the 75%-87% range at 550 nm, as listed in Table III.

Table III also shows that the color intensities of the PI hybrid films are affected by their organoclay content and that the PI hybrid films with lower organoclay contents had lower yellow indices (YIs) than those with higher organoclay contents. The YIs for the pure PI and the hybrid films with 10 wt% organoclay were 2.35 and 5.63, respectively. When the clay loading was increased to 20 and then to 40 wt%,

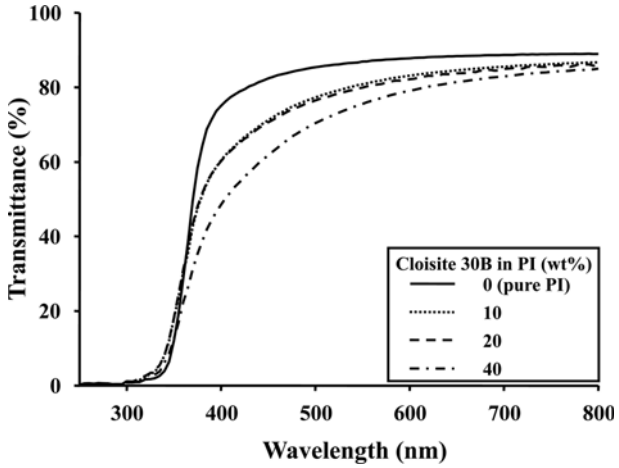

Figure 6. UV-Vis transmittance of PI hybrid films with various Cloisite 30B contents.

there were significant increases in the YIs to 6.23 and 13.15, respectively. However, these YIs are much lower than those for conventional aromatic PI films such as Kapton® 200KN (YI=97.50). By comparison, the hybrid film containing 40 wt% Cloisite 30B had a relatively high λ_0 and YI of 316 nm and 13.15, respectively, and the lowest optical transmittance of 75%, at 550 nm, as shown in Table III. These results suggest that this film has poor optical characteristics because of clay agglomeration for which evidence was found using XRD and TEM (Figures 1 and 2).

All the solvent-cast hybrid films with organoclay contents in the range 0-20 wt% were almost colorless and transparent, as shown in Figure 7((a)-(c)), which indicates that the addition of the organoclay to the PI matrix does not significantly

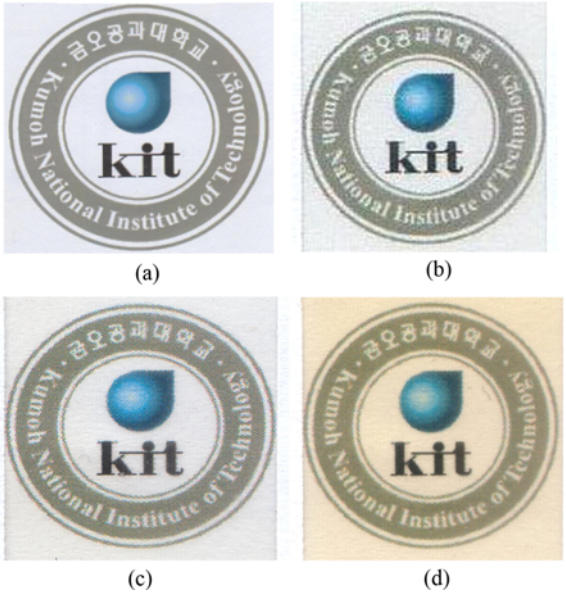

Figure 7. Photographs of PI hybrid films containing (a) 0 (pure PI), (b) 10, (c) 20, and (d) 40 wt% of Cloisite 30B.

Table IV. Gas Permeations of PI Hybrid Films

Organoclay (wt%)	Thickness (μm)	O_2TR^a (cc/m^2/day)	$P_c/P_p{}^b$
0 (pure PI)	74	768	1
10	72	42	0.05
20	71	28	0.04
40	68	18	0.02

[a]Oxygen transmission rate. [b]Composite permeability/polymer permeability (*i.e.*, relative permeability rate).

affect its transparency. These findings suggest that, even at an organoclay loading of 20 wt%, the phase domains in the hybrid film are significantly smaller than the wavelength of visible light (400-800 nm).[27] Thus, the hybrid films prepared in the present study exhibit excellent transparency because of the good dispersion of clay particles in the polymer matrix although the transparency does diminish slightly with increasing organoclay content because of agglomeration of the clay particles. Although the hybrid film containing 40 wt% Cloisite 30B appeared to be slightly yellow (Figure 7(d)), it was sufficiently transparent that letters could easily be seen through it.

Oxygen Permeation. It is well known that introducing an inorganic material into amorphous PI films affects their gas permeabilities.[31-33] The gas permeabilities of hybrid films are lower than those of pure polymer films and are independent of gas type. This behavior is easily understood if the matrix is capable of tight packing since the free volume, unoccupied space, is reduced, thereby decreasing its ability to transport permeants. Clearly, T_g is the critical factor in determining the maximum performance of polymer nanocomposites for barrier applications.[34,35] This phenomenon is also attributed to the high aspect ratio and the rigid clay platelets in the polymer matrix.

This paper describes the performance of barrier films containing aligned impermeable particles. We discuss our results in terms of relative permeability, P_c/P_p, where P_p is the permeability of the pure polymer and P_c is the permeability of the composite. The oxygen permeabilities for hybrid films with clay loadings of 0 to 40 wt% are summarized in Table IV. The permeability coefficient of the 10 wt% PI hybrid film was 95% (42 cc/m^2/day) lower than that of the pure PI film (768 cc/m^2/day). When the clay content was increased from 20 to 40 wt%, the relative O_2 permeability decreased linearly from 0.04 to 0.02 (from 28 to 18 cc/m^2/day). This reduced permeability is due to the large aspect ratios of dispersed clay layers in the polymer matrix, as has been shown in other research.[36-39]

Conclusions

We prepared and characterized colorless and transparent PI/Cloisite 30B hybrid films, using BTDA and m-BAPS mono-

mers by *in situ* solution intercalation *via* PAAs. The clay content of the hybrid films was varied from 10 to 40 wt%, and the effects of changes in clay content on the thermal property, morphology, optical transparency, and gas permeability of the films were examined.

The morphological results indicate that the dispersion in the PI matrix was better at a lower organoclay loading than at a higher one. Even at 20 wt% organoclay content, the clay particles were well dispersed in the matrix polymer without significant agglomeration of particles. The addition of organoclay into the PIs produced hybrid films with thermal- and gas-barrier properties superior to those of the pure PI polymer. However, the optical transparencies of the hybrid films were inferior to those of the pure PI film.

Acknowledgment. This research was supported by the Research Fund of Kumoh National Institute of Technology.

References

(1) W. Qu, T. Z. Ko, R. H. Vora, and T. S. Chung, *Polymer,* **42**, 6393 (2001).
(2) Y. C. Pang and H. W. Yang, U.S. Patent 6,093,790 (2000).
(3) S.-H. Hsiao, W. Guo, C. L. Ching, and W. T. Chen, *Eur. Polym. J.,* **46**, 1878 (2010).
(4) B. Y. Myung, J. S. Kim, and T. H. Yoon, *J. Polym. Sci. Part A: Polym. Chem.,* **41**, 3361 (2003).
(5) S. L. Ma, Y. S. Kim, J. H. Lee, J. S. Kim, I. Kim, and J. C. Won, *Polym. Korea,* **29**, 204 (2005).
(6) C. P. Yang, Y. Y. Su, S. J. Wen, and S. H. Hsiao, *Polymer*, **47**, 7021 (2006).
(7) C. P. Yang, Y. Y. Su, and Y. C. Chen, *J. Appl. Polym. Sci.*, **102**, 4101 (2006).
(8) U. Min and J.-H. Chang, *Polym. Korea,* **34,** 495 (2010).
(9) M. C. Choi, Y. K. Kim, and C. S. Ha, *Prog. Polym. Sci.,* **33**, 581 (2008).
(10) P. C. Wang and A. G. MacDiarmid, *Displays,* **28**, 101 (2007).
(11) P. E. Burrows, G. L. Graft, M. E. Gross, P. M. Martin, M. K. Shi, M. Hall, E. Mast, C. Bonham, W. Bennett, and M. B. Sullivan, *Displays,* **22**, 65 (2001).
(12) M. D. J. Auch, O. K. Soo, G. Ewald, and C. S. Jin, *Thin Solid Films,* **417**, 47 (2002).
(13) C. J. Chiang, C. Winscom, S. Bull, and A. Monkman, *Org. Electron.,* **10**, 1268 (2009).
(14) K. S. Yang, D. D. Edie, D. Y. Lim, Y. M. Kim, and Y. O. Choi, *Carbon*, **41**, 2039 (2003).
(15) J.-S. Park and J.-H. Chang, *Polym. Eng. Sci.,* **49**, 1357 (2009).
(16) K. Ghosal, B. D. Freeman, R. T. Chern, J. C. Alvarez, J. G. De la camoa, A. E. Lozano, and J. De Abajo, *Polymer*, **36**, 793 (1995).
(17) I. H. Choi, B. H. Sohn, and J. H. Chang, *Appl. Clay Sci.,* **48**, 117 (2010).
(18) M. Polverejan, T. R. Pauly, and T. J. Pinnavaia, *Chem. Mater.*, **12**, 2698 (2000).
(19) U. Min, J.-C. Kim, and J. H. Chang, *Polym. Eng. Sci.,* **51**, 2143 (2011).
(20) U. Min and J.-H. Chang, *J. Nanosci. Nanotechnol.,* **11**, 6404 (2011).
(21) J. S. Park and J. H. Chang, *Polym. Eng. Sci.,* **49**, 1357 (2009).
(22) D. Wang, J. Zhu, Q. Wao, and C. A. Wilie, *Chem. Mater.,* **14**, 3837 (2002).
(23) R. A. Vaia, K. D. Jandt, E. J. Kramer, and E. P. Giannelis, *Chem. Mater.,* **8**, 2628 (1996).
(24) I. H. Choi and J.-H. Chang, *Polym. Adv. Technol.,* **22**, 682 (2011).
(25) J.-H. Chang, B.-S. Seo, and D.-H. Hwang, *Polymer*, **43**, 2969 (2002).
(26) T. Agag and T. Takeichi, *Polymer*, **41**, 7083 (2000).
(27) T. D. Fornes, P. J. Yoon, D. L. Hunter, H. Keskkula, and D. R. Paul, *Polymer*, **43**, 5915 (2002).
(28) X. S. Petrovic, L. Javni, A. Waddong, and G. J. Banhegyi, *J. Appl. Polym. Sci*., **76**, 133 (2000).
(29) T. Agag, T. Koga, and T. Takeichi, *Polymer*, **42**, 3399 (2001).
(30) M. Okamoto, S. Morita, Y. H. Kim, T. Kotaka, and H. Tateyama, *Polymer*, **42**, 1201 (2001).
(31) J.-H. Chang, D. K. Park, and K. J. Ihn, *J. Appl. Polym. Sci*., **84**, 2294 (2002).
(32) K. Yano, A. Usuki, A. Okada, T. Kurauchi, and O. Kamigaito, *J. Polym. Sci. Part A: Polym. Chem. Ed.*, **31**, 2493 (1993).
(33) E. Picard, A. Vermogen, J. F. Gerard, and E. Espuche, *J. Memb. Sci.,* **292**, 133 (2007).
(34) S. S. Ray and M. Okamoto, *Prog. Polym. Sci*., **28**, 1539 (2003).
(35) J. H. Kim, W. J. Koros, and D. R. Paul, *Polymer*, **47**, 3104 (2006).
(36) T. Sakaya and N. Osaki, *J. Photopolym. Sci. Technol*., **19**, 197 (2006).
(37) B. Xu, Q. Zheng, Y. Song, and Y. Shangguan, *Polymer*, **47**, 2904 (2006).
(38) M. A. Osman, V. Mittal, M. Morbidelli, and U. W. Suter, *Macromolecules*, **36**, 9851 (2003).
(39) J. Masuda and M Ohkura, *J. Appl. Polym. Sci*., **106**, 4031 (2007).